

Influence of confinement on single-electron charging in a network of nanoparticles

S. Sarkar Pal,^{a)} K. Schouteden, and C. Van Haesendonck,

Laboratory of Solid-State Physics and Magnetism, Katholieke Universiteit Leuven, Celestijnenlaan 200D, BE-3001 Leuven, Belgium

(Received 13 May 2011; accepted 14 July 2011; published online 25 August 2011)

We investigated the single-electron tunneling (SET) behavior in a network of ligand stabilized Au nanoparticles (NPs) that are self-organized on an Au(111) surface by means of low-temperature scanning tunneling microscopy and spectroscopy. We demonstrate that for a proper combination of ligand chain length and NP radius the ligand shell is able to isolate a particle from the neighboring ones. This results in SET spectra with a clear Coulomb blockade and a regular staircase, similar to SET spectra obtained for isolated particles. A fraction of the investigated particles exhibits additional fine structure on top of the Coulomb charging peaks in the tunneling conductance spectra. The origin of the fine structure can be related to quantum size effects due to the very small NP size rather than to inter-particle capacitive coupling. Our findings indicate the possibility of using an individual particle in the self-organized network as the central Coulomb island in a double-barrier tunnel junction configuration, similar to the case of an isolated particle. © 2011 American Institute of Physics. [doi:10.1063/1.3624952]

I. INTRODUCTION

The single-electron tunneling (SET) device is considered as a possible key component for future quantum electronics. A powerful fabrication technique for designing SET devices relies on self-assembly, where organic molecules are used to attach a metallic or semiconducting nanoparticle (NP) to electrodes.¹ Chemically synthesized and ligand stabilized NPs are increasingly used as the central island in a double-barrier tunnel junction (DBTJ) geometry.^{2–7} The ligand shell acts as a tunnel barrier, thus isolating the NP from the electrodes. For sufficiently small particles the discrete nature of electron charge results in discrete charging energies and SET behavior. At the same time, quantum confinement of the electrons gives rise to discrete energy levels that can have a significant effect on the SET behavior.^{2,5,8–10} While the case of an isolated single metallic NP in a DBTJ configuration has been investigated in detail,^{2,5,8,11} similar research on the SET and quantum confinement behavior for a network of NPs, where the coupling with the neighboring particles can become significant, still presents important challenges.

Here, we report on our scanning tunneling microscopy (STM) and scanning tunneling spectroscopy (STS) investigation of a network of ligand-stabilized metallic NPs that are self-organized on an Au(111) substrate. The conductance spectra observed before for NP networks either showed an irregular staircase-like structure with non-equidistant steps and different widths,^{12,13} or a negative differential resistance effect,^{14,15} which were attributed to inter-particle tunneling. An obvious question is therefore whether an individual NP in the network can serve as the central Coulomb island in a

DBTJ configuration with the STM tip and the metal substrate acting as the two electrodes. We demonstrate that for a proper combination of ligand chain length and NP radius the ligand shell is able to isolate a particle from the neighboring particles, resulting in SET spectra with clear Coulomb blockade (CB) and regular Coulomb staircase (CS). The spectra can be tuned within a certain range by adjusting the separation between STM tip and NP. Splitting of charging peaks is observed in several cases, similar to earlier observations on isolated particles. The origin of the fine structure is discussed in detail, taking into account both the discreteness of the Au NP energy levels and the inter-particle coupling.

II. EXPERIMENTAL DETAILS

Epitaxially grown 140 nm thick Au(111) films on freshly cleaved mica were prepared *ex situ* by molecular beam epitaxy at elevated temperatures.¹⁶ The resulting films consist of atomically flat islands with dimensions up to 500×500 nm². We used octanethiol [$\text{CH}_3(\text{CH}_2)_7\text{SH}$] functionalized Au NPs (Sigma-Aldrich), hereafter referred to as OFAuNPs. The particles have an Au core diameter in the 2 to 4 nm range, with an average diameter of 2.8 nm. Including the alkanethiol capping molecules with chain length of 1.02 nm,¹⁷ the average diameter of the NP is around 4.8 nm. In order to obtain a monolayer of OFAuNPs on the Au(111) surface, the Au(111) substrate was immersed in a toluene solution of OFAuNPs (1 mg/ml) for about 12 hs. Next, the sample was blown dry under nitrogen flow. STM and STS measurements were performed with a commercially available STM setup (Omicron NanoTechnology) at a base pressure in the 10^{-11} mbar range and at liquid helium temperature ($T_{\text{sample}} \simeq 4.5$ K). Mechanically cut PtIr (10% Ir) tips were used. STM topographic imaging is performed in constant current mode. Simultaneously, local spectroscopy data (tunneling current I versus

^{a)} Author to whom correspondence should be addressed. Electronic mail: sudipta.sarkar12@gmail.com. Present address: Central Scientific Instruments Organisation, Sector 30C, Chandigarh 160030, India.

tunneling voltage V with open feedback loop) are acquired. At each position a number of spectra is collected at different tip-sample separation by varying the setpoint tunneling current (I_{set}). It should be noted that stable topography images can only be recorded within a limited range of tunneling current and voltage setpoints. On the other hand, highly stable I - V spectra can be obtained within a broad range of setpoints after zooming in on a region of about $0.5 \times 0.5 \text{ nm}^2$ on top of an NP. The STM tip is hence always located near the NP center during the recording of the I - V spectrum, i.e., well away from the edges of the particle.

III. RESULTS AND DISCUSSION

A schematic view of the monolayer and the corresponding DBTJ configuration are presented in Fig. 1(a) and Fig. 1(b), respectively. A typical STM topographic image of self-assembled OFAuNPs on Au(111) is presented in Fig. 1(c). The NPs homogeneously form a complete monolayer all over the entire substrate. Individual particles without surrounding neighbors cannot be retrieved. In the upper part of the STM topographic image in Fig. 1(c), the particles can be observed to adapt a hexagonal packing. It was observed before that similar alkanethiol capped Au nanoparticles form long-range ordered hexagonal arrays.^{18,19} Here, the NP size distribution as well as the steps on the Au(111) surface may inhibit the particles from forming a more perfect hexagonal packing. The height profiles [Fig. 1(d)] reveal a height variation around 1.4 nm and an average nearest neighbor particle distance around 5 nm, which is close to the average OFAuNP diameter of 4.8 nm. We may, therefore, conclude that the capping octanethiol molecules of neighboring nanoparticles are not interweaving and that the Au cores are well isolated from each other after deposition. This allows us to probe the electronic properties of single particles by means of STS.

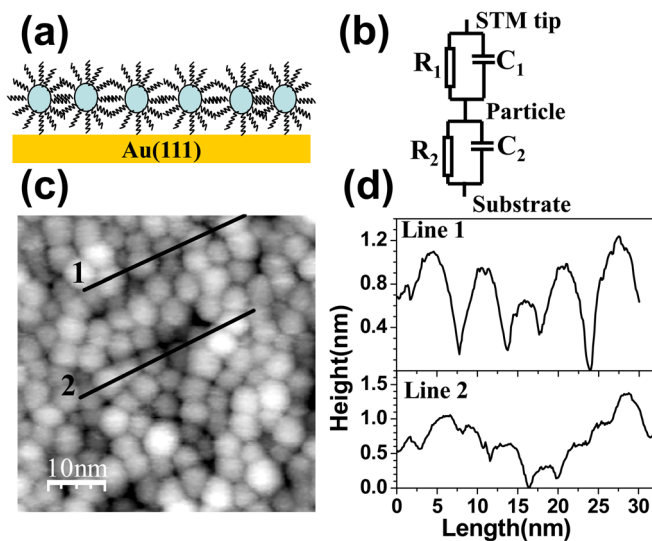


FIG. 1. (Color online) (a) Schematic diagram of an OFAuNP monolayer on the Au(111) substrate. (b) Equivalent electric circuit for an STM measurement. (c) A typical topography STM image of an OFAuNP monolayer ($I_{set} = 0.05 \text{ nA}$, $V_{set} = 1.5 \text{ V}$). (d) Height profiles taken along the black lines in panel (c).

All investigated NPs are found to exhibit a clear CB around $V=0$ and a CS at higher V in the I - V spectra. Because of the distribution in particle size, the CB gap (V_{CB}) was found to vary depending on the particle size, e.g., from 300 meV to 360 meV for $I_{set} = 3 \text{ nA}$ and $V_{set} = 1 \text{ V}$. In Fig. 2, a series of I - V curves is presented for a 2 nm particle at various tip-particle separations obtained by adjusting I_{set} . The charging energy of the system is given by $e^2/2C_{total}$ where C_{total} is the total capacitance of the particle with respect to its environment, including the electrodes.²⁰ According to the orthodox theory²¹ the width of the gap resulting from the CB, i.e., the width of the zero conductance region in the I - V curve is given by $V_{CB} = e/[\max(C_1, C_2)]$ if the residual charge Q_0 is very small.²² C_1 and C_2 are the capacitances of the tip-particle and particle-substrate tunnel junctions, respectively [Fig. 1(b)]. The capacitance C_1 depends on the tip-particle separation d_1 , which can be adjusted by changing I_{set} (keeping V_{set} constant). When I_{set} increases (d_1 decreases), we find that V_{CB} remains unchanged within the investigated range $0.5 \text{ nA} < I_{set} < 30 \text{ nA}$. Since C_2 does not depend on the tip position, this indicates that C_2 is the dominating capacitance in our experiments. On the other hand, we observe prominent CSs in the I - V spectra only for higher I_{set} ($>10 \text{ nA}$). Prominent CSs are expected only when either $C_1R_1/C_2R_2 \gg 1$ or $C_2R_2/C_1R_1 \gg 1$. In our case, $C_2 > C_1$. The condition for the appearance of a CS will not be satisfied for lower I_{set} values, i.e., larger tip-particle separations that imply $R_1 > R_2$, but with R_1 and R_2 being still of the same order of magnitude. When I_{set} increases, the tip will come in contact with the end group of the alkanethiol molecule that protects the NP, resulting in a symmetric DBTJ with $R_1/R_2 = 1$. With further increase of I_{set} , the tip will start to penetrate the protecting molecule, finally resulting in a ratio $R_1/R_2 \ll 1$. In the upper inset of Fig. 2, we plot the calculated I - V spectra of a DBTJ with $C_1/C_2 = 0.5$ following

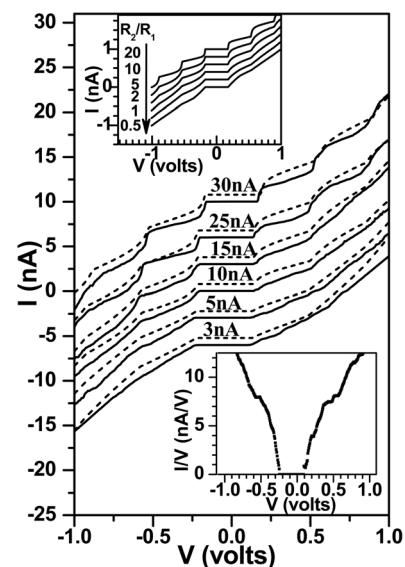


FIG. 2. Typical I - V curves (solid lines) and corresponding fitted curves (dotted lines) for a 2 nm OFAuNP for different I_{set} ($V_{set} = 1 \text{ V}$). Curves are shifted vertically for clarity. Upper inset: Calculated I - V curves for different R_2/R_1 ratio with $C_1/C_2 = 0.5$. Lower inset: Variation of I/V with V ($I_{set} = 0.5 \text{ nA}$, $V_{set} = 1 \text{ V}$).

orthodox theory.^{21,22} The calculation shows that a prominent CS indeed gradually appears with increasing R_2/R_1 ratio.

We also fitted the experimental curves that are presented in the main panel of Fig. 2. C_2 and R_2 are found to be around 0.45 aF and 90 M Ω , respectively, regardless of the tip-OFAuNP separation d_1 . This is consistent with the assumption that the particle-substrate junction is not affected by the tip position. It can be observed in the lower inset of Fig. 2, that the quantity I/V varies approximately linearly with V for V exceeding V_{CB} , indicating that I is a quadratic function of V . This nonlinearity can be related to the non-ideality of the tunnel barriers formed by the capping molecules,²³ as well as to variations in the barrier height or the density of states, inelastic tunneling and many-body excitations.²⁴ To take this non-linear variation of the current into account, Zabet-Khosousi *et al.* proposed a V -dependent junction resistance $R_j(V) = R_{0j}/(1 + \alpha|V - V_{CB}|)$, where R_{0j} is the junction resistance assuming a linear I - V and α is the nonlinearity parameter.²³ The values for C_1 , C_2 , R_{01} , R_{02} , Q_0 and α obtained from fitting the experimental curves of Fig. 2 are listed in Table I.

The resistance R_{02} of the particle-substrate tunnel barrier that consists of octanethiol molecules is found to be around 90 M Ω (Table I). The resistance of a single octanethiol molecule was reported before by Xu *et al.* to be 50 M Ω (Ref. 25) and by Kockmann *et al.* to be 100–150 M Ω ,²⁶ i.e., comparable to our result. We would like to point out that in our case the self-capacitance C_{self} of the central island^{20,27,28} is comparable to the junction capacitance $C_{1(2)}$ obtained by fitting of the experimental data. For particles of diameter $2r$ in the 2 to 3 nm range, passivated with an organic shell of thickness (δ) 1.4 nm and dielectric constant (ϵ) 2.7, C_{self} is found to vary between 0.5 and 0.9 aF when using the expression $C_{self} = 4\pi\epsilon\epsilon_0 r(1 + \frac{\delta}{r})$ with ϵ_0 the permittivity of free space. As proposed by Ohgi *et al.*, the value of $C_{1(2)}$ obtained by fitting is not the pure junction capacitance, but corresponds to $C_{1(2)} = [C_{total}C'_{1(2)}]/(C'_1 + C'_2)$ (Ref. 20), where C'_1 and C'_2 are the pure junction capacitance between tip and particle and between particle and substrate, respectively, and $C_{total} = C_{self} + C'_1 + C'_2$.

In addition to the main CS steps, additional step-like features are observed in I - V spectra for a significant fraction of OFAuNPs [Fig. 3(a)], irrespective of the particle diameter. These extra features can be observed as multiple peaks in the corresponding dI/dV curves [Fig. 3(b)]. The appearance of multiple peaks can be attributed either to the discrete character of the energy levels of the OFAuNPs or to inter-particle tunneling. For a 3.0 nm Au NP the average level spacing δE

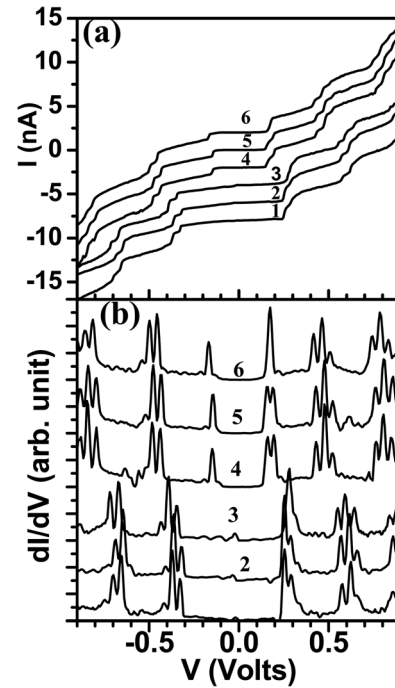


FIG. 3. Fine structure can be observed in panel (a) I - V curves and panel (b) corresponding dI/dV curves for different OFAuNPs ($V_{set} = 1$ V). Curves 1, 2 and 3 are obtained for a 3.0 nm OFAuNP at $I_{set} = 10$ nA, 12 nA and 15 nA, respectively. Curves 4 and 5 are obtained for a 3.5 nm OFAuNP at $I_{set} = 10$ nA and 15 nA, respectively. Curve 6 is obtained for a 2 nm OFAuNP at $I_{set} = 10$ nA.

is expected to be around 15 meV following the independent electron particle-in-a-box model¹⁰: $\delta E = (2\pi^2\hbar^2)/(mk_F\nu)$, where ν is the volume of the particle, m is the electron mass and k_F is the Fermi wave vector [≈ 12.0 nm⁻¹ for Au (Ref. 3)]. The experimentally observed average spacing between the multiple peaks (taking into account the capacitive voltage division^{8,16}) is around 15 meV, in agreement with the predicted theoretical value.

In order to be able to resolve the additional fine structure resulting from the discrete energy states, the following conditions need to be satisfied.¹⁰ First, to avoid thermal smearing $k_B T \ll \delta E$, which is satisfied at $T \approx 4.5$ K. Second, the tunneling rate Γ^{tun} out of a discrete state of the metal particle into the STM tip or the substrate has to be sufficiently small so that the tunneling-induced level widths $\hbar\Gamma^{tun}$ do not cause neighboring levels to overlap, i.e., $\hbar\Gamma^{tun} \ll \delta E$. Γ^{tun} varies inversely proportional to $R_{1(2)}$, which we found to be of the order of $10^6 \Omega$ from the curve fitting. The corresponding contribution to the level width $\hbar\Gamma^{tun}$ (with Γ^{tun} of the order of 10^{11} s⁻¹ obtained using the expression of the tunneling rate in Ref. 21) is then around 0.1 meV. Consequently, the above mentioned two criteria are satisfied for our STS experiments. We simulated the experimental results (see Fig. 4) using orthodox theory, assuming that the discrete energy states of the NP are equally spaced.²¹ It can be seen that the simulated curve qualitatively reproduces the fine structure around the main charging peaks. However, it does not reproduce all details of the experimental curve. While the discrete level spacing of a NP is commonly estimated using the independent electron particle-in-a-box model, the different peaks may not directly reflect independent-electron states. It is,

TABLE I. Overview of the parameters obtained from fitting of the experimental STS spectra by orthodox theory.

I_{set} (nA)	C_1 (aF)	C_2 (aF)	R_{01} (M Ω)	R_{02} (M Ω)	Q_0	α
30	0.35	0.45	4.95	90	0.02e	0.2
25	0.26	0.45	8.95	90	-0.1e	0.2
15	0.24	0.45	20.0	90	-0.1e	0.5
10	0.18	0.45	65.0	90	-0.1e	0.5
5	0.12	0.45	90.0	90	-0.13e	1.5
3	0.09	0.45	95.0	90	-0.05e	1.0

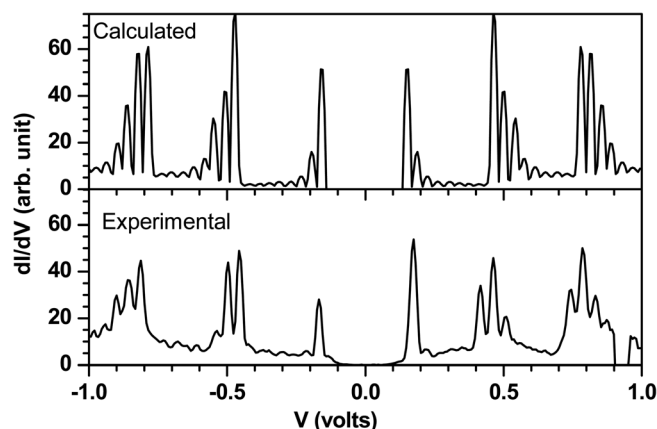


FIG. 4. Experimental dI/dV curve of a single OFAuNP and the corresponding simulated dI/dV curve that takes into account the discrete nature of the electronic structure of the OFAuNP.

therefore, important to note that the simulation does not take into account the electron-electron interaction effects, which may become important for very small particles.^{5,29,30}

Since we are dealing with a network of NPs rather than with one isolated NP, tunneling through neighboring particles needs to be considered. Parthasarathy *et al.* previously investigated the impact of structural disorder on electronic transport in alkanethiol stabilized gold nanocrystal networks.^{31,32} They concluded that the alkanethiol ligands simply act as mechanical spacers and do not introduce additional states in the tunneling barrier between two neighboring nanocrystals, which is too high to be thermally hopped over. As a result, there only exists weak coupling between two neighboring nanocrystals in the network. Earlier reports for Au/ Al_2O_3 granular films¹² and for monolayer of decanethiol capped Ag NPs¹³ have indicated that tunneling via neighboring particles results in irregular staircase-like features with non-equidistant steps and different widths in the conductance spectra. The ratio of the capacitances between particle and substrate (C_2) and between two neighboring particles (C_{ij}) determines whether the tunneling occurs directly through the DBTJ formed by the tip-particle-substrate system and/or through a “triple” junction formed by the tip-particle-neighboring particles-substrate. We may therefore conclude that there is no significant contribution from tunneling through neighboring particles for OFAuNPs on which we observe a regular CS with a well-defined charging period (see Fig. 2). Only if $C_{ij} > C_2$, the blockade for tunneling through neighboring particles becomes sufficiently small to open this channel for electron flow.¹⁵ C_2 (C_{ij}) is inversely proportional to the NP-substrate distance d_2 (distance to the neighboring NP d_{ij}), which depends on the chain length of the ligand molecules. In our configuration $d_{ij} \geq d_2$. Equality arises when the hydrocarbon chains of the neighboring particles are fully interdigitated. As already discussed above, we can infer from our STM images that the center to center distance between two neighboring NPs of average diameter (2.8 nm) is 5.0 nm, implying d_{ij} is larger than the distance d_2 that is determined by the octanethiol chain length [= 1.02 nm (Ref. 17)]. The inter-particle capacitance C_{ij} is therefore smaller than the NP-substrate capacitance C_2 .

It has been reported before that charging peaks can split into doublets in a double quantum dot system, where the peak separation increases with increasing inter-particle coupling.³³ The coupling between two neighboring particles is inversely proportional to the ratio of the inter-particle separation and the particle diameter.^{34,35} Therefore, two NPs with bigger radii will have stronger inter-particle coupling when compared to two smaller NPs, provided the molecular spacer between the NPs is the same. It can, hence, be expected that larger particles (with stronger inter-particle coupling) will show more prominent extra peaks when compared to the smaller particles. Here, the extra fine peaks are observed irrespective of particle radius [Fig. 3(b)] and the energy separation of the peaks increases with decreasing particle radius [Fig. 3(b)]. We may therefore, conclude that in our case the extra peaks are related to discreteness of the energy states of the OFAuNPs, rather than to inter-particle tunneling. Further experiments are in progress, where we rely on a mixed thiol-dithiol molecular layer to attach well separated individual OFAuNPs to the substrate.¹⁶ Varying the thiol to dithiol ratio then provides ultimate control over the OFAuNP coverage, which will allow us to systematically compare the conductance spectra for an isolated OFAuNP to that for an OFAuNP network.

IV. SUMMARY AND CONCLUSIONS

In summary, preformed octanethiol capped Au NPs were observed to self-organize in an ordered and densely packed overlayer on Au(111) substrates. STS spectra measured by positioning the STM tip on a single particle revealed the presence of pronounced CBs and CSs. Splitting of the charging peaks was observed in several cases. For our combination of ligand chain length and NP radius the inter-particle capacitance is smaller than the particle-substrate capacitance. The charging energy for tunneling through neighboring particles is therefore larger than the charging energy for the tip-particle-substrate path, implying that the former channel is blocked for electron tunneling. As a result, inter-particle capacitive coupling, which depends on the ratio of the inter-particle separation to the particle diameter, does not dominate the conductance spectra in our experiments. Our findings indicate that an individual particle in the self-organized network can be used as the central Coulomb island in a double-barrier tunnel junction configuration, similar to the case of an isolated particle.

ACKNOWLEDGMENTS

This work has been supported by the Research Foundation - Flanders (FWO, Belgium) as well as by the Flemish Concerted Action (Grant No. GOA/2004/02) and the Belgian Interuniversity Attraction Poles (Grant No. IAP/P6/42) research programs. K.S. is a postdoctoral researcher of the FWO.

¹D. M. Adams, L. Brus, C. E. D. Chidsey, S. Creager, C. Creutz, C. R. Kagan, P. V. Kamat, M. Lieberman, S. Lindsay, R. A. Marcus, *J. Phys. Chem. B* **107**, 6668 (2003).

²U. Banin, Y. Cao, D. Katz, and O. Millo, *Nature* **400**, 542 (1999).

- ³B. Wang, H. Wang, H. Li, C. Zeng, J. G. Hou, and X. Xiao, *Phys. Rev. B* **63**, 035403 (2000).
- ⁴H. Zhang, G. Schmid, and U. Hartmann, *Nano Lett.* **3**, 305 (2003).
- ⁵B. Wang, K. Wang, W. Lu, J. Yang, and J. G. Hou, *Phys. Rev. B* **70**, 205411 (2004).
- ⁶H. Zhang, Y. Yasutake, Y. Shichibu, T. Teranishi, and Y. Majima, *Phys. Rev. B* **72**, 205441 (2005).
- ⁷S. Pradhan, J. Sun, F. Deng, and S. Chen, *Adv. Mater.* **18**, 3279 (2006).
- ⁸J. G. A. Dubois, J. W. Gerritsen, S. E. Shafranjuk, E. J. G. Boon, G. Schmid, and H. van Kempen, *Europhys. Lett.* **33**, 279 (1996).
- ⁹O. Millo, D. Katz, Y. Cao, and U. Banin, *Phys. Rev. B* **61**, 016773 (2000).
- ¹⁰J. Von Delft and D. C. Ralph, *Phys. Rep.* **345**, 61 (2001).
- ¹¹D. Davidović and M. Tinkham, *Phys. Rev. B* **61**, R16359 (2000).
- ¹²E. Bar-Sadeh, Y. Goldstein, C. Zhang, H. Deng, B. Abeles, and O. Millo, *Phys. Rev. B* **50**, 8961 (1994).
- ¹³G. Medeiros-Ribeiro, D. A. A. Ohlberg, R. S. Williams, and J. R. Heath, *Phys. Rev. B* **59**, 1633 (1999).
- ¹⁴B. Wang, K. Wang, W. Lu, H. Wang, Z. Li, J. Yang, and J. G. Hou, *Appl. Phys. Lett.* **82**, 3767 (2003).
- ¹⁵H. Zhang, D. Mautes, and U. Hartmann, *Nanotechnology* **18**, 065202 (2007).
- ¹⁶K. Schouteden, N. Vandamme, E. Janssens, P. Lievens, and C. Van Haesendonck, *Surf. Sci.* **602**, 552 (2008).
- ¹⁷J. F. Hicks, A. C. Templeton, S. Chen, K. M. Sheran, R. Jasti, R. W. Murray, J. Debord, T. G. Schaaff, and R. L. Whetten, *Anal. Chem.* **71**, 3703 (1999).
- ¹⁸T. P. Bigioni, L. E. Harrell, W. G. Cullen, D. K. Guthrie, R. L. Whetten, and P. N. First, *Eur. Phys. J. D* **6**, 355 (1999).
- ¹⁹H. Osman, J. Schmidt, K. Svensson, R. E. Palmer, Y. Shigeta, and J. P. Wilcoxon, *Chem. Phys. Lett.* **330**, 1 (2000).
- ²⁰T. Ohgi and D. Fujita, *Phys. Rev. B* **66**, 115410 (2002).
- ²¹M. Amman, R. Wilkins, E. Ben-Jacob, P. D. Maker, and R. C. Jaklevic, *Phys. Rev. B* **43**, 1146 (1991).
- ²²A. E. Hanna and M. Tinkham, *Phys. Rev. B* **44**, 5919 (1991).
- ²³A. Zabet-Khosousi, Y. Suganuma, K. Lopata, P.-E. Trudeau, A.-A. Dhirani, and B. Statt, *Phys. Rev. Lett.* **94**, 096801 (2005).
- ²⁴R. Wilkins, E. Ben-Jacob, and R. C. Jaklevic, *Phys. Rev. Lett.* **63**, 801 (1989).
- ²⁵B. Xu and N. J. Tao, *Science* **301**, 1221 (2003).
- ²⁶D. Kockmann, B. Poelsema, and H. J. W. Zandvliet, *Nano Lett.* **9**, 1147 (2009).
- ²⁷C. A. Berven and M. N. Wybourne, *Appl. Phys. Lett.* **78**, 3893 (2001).
- ²⁸A. Bezryadina, C. Dekker, and G. Schmid, *Appl. Phys. Lett.* **71**, 1273 (1997).
- ²⁹B. L. Altshuler, Y. Gefen, A. Kamenev, and L. S. Levitov, *Phys. Rev. Lett.* **78**, 2803 (1997).
- ³⁰D. C. Ralph, C. T. Black, and M. Tinkham, *Physica B* **218**, 258 (1996).
- ³¹R. Parthasarathy, X.-M. Lin, and H. M. Jaeger, *Phys. Rev. Lett.* **87**, 186807 (2001).
- ³²R. Parthasarathy, X.-M. Lin, K. Elteto, T. F. Rosenbaum, and H. M. Jaeger, *Phys. Rev. Lett.* **92**, 076801 (2004).
- ³³F. R. Waugh, M. J. Berry, D. J. Mar, R. M. Westervelt, K. L. Campman, and A. C. Gossard, *Phys. Rev. Lett.* **75**, 705 (1995).
- ³⁴G. Markovich, C. P. Collier, and J. R. Heath, *Phys. Rev. Lett.* **80**, 3807 (1998).
- ³⁵H. Liu, B. S. Mun, G. Thornton, S. R. Isaacs, Y.-S. Shon, D. F. Ogletree, and M. Salmeron, *Phys. Rev. B* **72**, 155430 (2005).